Mechanisms of winter precipitation variability in the European-Mediterranean region associated with the North Atlantic Oscillation

Richard Seager *, Haibo Liu, Yochanan Kushnir

Lamont Doherty Earth Observatory of Columbia University, Palisades, New York

Timothy J. Osborn

Climatic Research Unit, School of Environmental Sciences, University of East Anglia, Norwich, United Kingdom

Isla R. Simpson

National Center for Atmospheric Research, Boulder, CO

Colin R. Kelley

International Research Institute for Climate and Society, Columbia University, Palisades, New York

Jennifer Nakamura

Lamont Doherty Earth Observatory of Columbia University, Palisades, New York

Early Online Release: This preliminary version has been accepted for publication in *Journal of Climate*, may be fully cited, and has been assigned DOI 10.1175/JCLI-D-20-0011.1. The final typeset copyedited article will replace the EOR at the above DOI when it is published.

*Corresponding author address: Richard Seager, Lamont Doherty Earth Observatory of Columbia University, 61 Route 9W, Palisades, NY 10964

Submitted to *J. Climate*, January 2020.

E-mail: seager@ldeo.columbia.edu

Accepted for publication in *Journal of Climate*. DOI 10.1175/JCLI-D-20-0011.1.

ABSTRACT

The physical mechanisms whereby the mean and transient circulation anomalies associated with the North Atlantic Oscillation (NAO) drive winter mean precipitation anomalies across the North Atlantic, Europe and the Mediterranean are investigated using the European Centre for Medium Range Weather Forecasts Interim Reanalysis. A moisture budget decomposition is used to identify the contribution of the anomalies in evaporation, the mean flow, storm tracks and the role of moisture convergence and advection. Over the eastern North Atlantic, Europe and the Mediterranean, precipitation anomalies are primarily driven by the mean flow anomalies with, for a positive NAO, anomalous moist advection causing enhanced precipitation in the northern British Isles and Scandinavia and anomalous mean flow moisture divergence causing drying over continental Europe and the Mediterranean region. Transient eddy moisture fluxes work primarily to oppose the anomalies in precipitation minus evaporation generated by the mean flow but shifts in storm track location and intensity help explain regional details of the precipitation anomaly pattern. The extreme seasonal precipitation anomalies that occurred during the two winters with the most positive (1988/89) and negative (2009/10) NAO indices are also explained by NAO-associated mean flow moisture convergence anomalies.

Accepted for publication in *Journal of Climate*. DOI 10.1175/JCLI-D-20-0011.1.

1. Introduction

The North Atlantic Oscillation (NAO) is a seesaw in pressure between the subpolar Icelandic Low and the subtropical Azores High regions of the North Atlantic Ocean. The impacts of anomalies in the strength of the Icelandic Low on temperatures in Greenland and Denmark had been noticed as far back as the 1770s (see van Loon and Rogers (1978)). When the Icelandic Low is strong, cyclonic flow brings cold northerly air to Greenland and warm southerly air to northwestern Europe creating a west-east seesaw in temperature. A significant advance in dynamical understanding of the NAO came through the use of correlation analyses of meteorological records from multiple widely spread weather stations. Walker and Bliss (1932) created an NAO index that used sea level pressure (SLP) and temperature data from stations around the North Atlantic and into Europe. They published maps of SLP and temperature correlations with this index for December to February. The maps show the NAO to be a hemispheric scale phenomenon with, in its positive phase, high SLP spanning across the subtropics and mid-latitudes from the Americas to western Asia and low SLP spanning from eastern Canada across the subpolar North Atlantic to Scandinavia. Notably, Walker and Bliss (1932) also mapped precipitation anomalies which showed, again for the positive phase of the NAO, increased precipitation in Scandinavia, reduced precipitation over most of continental Europe and the western and central Mediterranean and increased precipitation over the Levant.

Modern work has greatly improved characterization and understanding of the NAO. It is now known to fundamentally arise from the internal atmospheric dynamics of wave-wave and/or wave-mean flow interaction. This is consistent with the stationary wave anomalies that define the NAO being strongly associated with anomalies in the location and intensity of the North Atlantic storm track (Rogers 1997). During the positive phase of the NAO the storm track is intensified over

Accepted for publication in *Journal of Climate*. DOI 10.1175/JCLI-D-20-0011.1.

Scandinavia and weakened over southern Europe and vice versa for the negative phase of the NAO. Also consistent with the idea of an origin in wave-wave interaction is that the NAO has considerable power at the synoptic timescale (Feldstein 2000). Further, it has been shown that interannual variability of the NAO can be explained in terms of such climate "noise" and does not require forcing external to the atmosphere (Feldstein 2000).

Different ideas have been proposed for how wave-wave and/or wave-mean flow interaction generate the NAO. DeWeaver and Nigam (2000) emphasized a two-way constructive interaction between the zonal mean flow and fluxes of vorticity and heat by the stationary waves that could explain the NAO and its persistence. In contrast, Barnes and Hartmann (2010), examining the circulation over the Atlantic sector only, argued that the stationary wave anomaly of the NAO caused a shift in the jet stream and the location of transient eddy generation which generated vorticity fluxes that reinforced the stationary wave - a wave-wave interaction. They also show that the induced vertical circulation and low level divergent flow maintained the flow anomaly against surface damping leading to persistence. These mechanisms are not mutually exclusive. The negative NAO phase is also associated with increased blocking frequency in the northwest Atlantic region which might also be indicative of coupling between synoptic and seasonal timescale eddies (Croci-Maspoli et al. 2007). Also it has become clear that variability of the NAO on weather and seasonal timescales is strongly influenced by downward propagation, on a timescale of weeks, of anomalies in the stratospheric polar vortex (e.g. Baldwin and Dunkerton (2001)). As discussed in the comprehensive, informative review by Kidston et al. (2015), the stratospheric influence on the extratropical troposphere, including the NAO, extends across all timescales and works by initiating the wave-wave and wave-mean flow feedbacks discussed above.

Despite these understandings of flow anomalies on the subseasonal timescale, there remains considerable disputation about the sources of interannual to multidecadal variability of the NAO.

Accepted for publication in *Journal of Climate*. DOI 10.1175/JCLI-D-20-0011.1.

This variability is quite marked with a trend towards a negative NAO from the 1920s to the 1960s, followed by a positive trend to the 1990s, a negative trend to about 2010 and another upward trend since (see Hurrell (1995); Pinto and Raible (2012) and Figure 1). Using very different approaches, both Feldstein (2002) and Osborn (2004) argued that the late 20th century increase of the NAO could not be explained by internal atmosphere variability and required some forcing, either from the oceans and cryosphere or radiative. For a while it was thought that the late 20th century upward trend of the NAO might be a response to rising greenhouse gas concentrations (e.g. Shindell et al. (1999)). However, the subsequent decline in the NAO, together with awareness that, according to coupled models, forced changes to date are small compared to the observed variability (Osborn 2011), has renewed efforts to explain where the impressive decadal variability originates from. It has been argued that SST forcing of the NAO, primarily from the tropical Pacific, but potentially involving the stratosphere (Ineson and Scaife 2009), and the solar irradiance influence on the stratospheric polar vortex enable skillful prediction of the NAO on seasonal to interannual timescales (Scaife et al. 2014). However, it should be noted that current coupled models fail to simulate the degree of low frequency variability that has been observed (Kravtsov 2017; Wang et al. 2017; Kim et al. 2018; Simpson et al. 2018). This is not due to the historical record being unusual since decadal and even longer timescale variability of the NAO is robust in multi-century instrumental (Mellado-Cano et al. 2019) and tree ring-based (Cook et al. 2019) estimates of the NAO.

The precipitation anomalies associated with the NAO have considerable social impacts. For example, it has been shown that the NAO has a strong influence on the occurrence of extreme precipitation at the daily timescale in the western Mediterranean and northwestern Europe (Krichak et al. 2014). The NAO significantly influences river flows in the Middle East and, hence, water availability for agriculture, power generation and urban populations (Cullen et al. 2002), water

Accepted for publication in *Journal of Climate*. DOI 10.1175/JCLI-D-20-0011.1.

availability for intensive agriculture and hydropower in the Iberian peninsula (Trigo et al. 2004), wind power and solar potential over Iberia (Jerez et al. 2013), hydropower output in Norway (Cherry et al. 2005) and wheat yields in Europe and North Africa (Anderson et al. 2019). All these examples of social impacts of the NAO follow primarily from how the NAO influences precipitation variability in the winter season. While our knowledge of the dynamics of NAO variability is incomplete, we know even less about the physical mechanisms of the associated precipitation variability. Typically, authors simply state that NAO variability generates precipitation anomalies via shifts in winds and storm tracks but do not state how these shifts contribute, what their spatial patterns are or their relative amplitude. Here, to the best of our knowledge, we provide the first comprehensive, quantitative assessment of how the NAO generates precipitation anomalies. In a solely observational study, we quantify the mechanisms using a well established (Seager et al. 2010b) decomposition of the moisture budget in an atmospheric reanalysis. This will allow us to assess how precipitation variations across the North Atlantic, Europe and Mediterranean region are related to changes in circulation and humidity, changes in mean flow moisture convergence and advection and changes in storm tracks. We will also examine for two winters with NAO extremes the mechanisms of associated precipitation extremes and the NAO contribution. Collectively, this will provide a more complete understanding of NAO-related precipitation variability.

2. Data and Methodology

a. Reanalysis and observational data sets

To evaluate the mechanisms of NAO-related precipitation variability we use the European Centre for Medium Range Weather Forecasts Interim Reanalysis (ERA-Interim) at 6-hourly resolution for the period January 1979 to December 2017. To compare the precipitation anomalies in ERA-

Accepted for publication in *Journal of Climate*. DOI10.1175/JCLI-D-20-0011.1.

Interim against observations for specific extremes of the NAO, and to compare histories of the NAO and observed precipitation around the Europe and Mediterranean region, we use the National Oceanic and Atmospheric Administration Climate Prediction Centre (CPC) Merged Analysis of Precipitation (CMAP, Xie and Arkin (1996, 1997)). CPC CMAP is a merge of satellite and gauge-based data and hence provides values over ocean as well as land and cover January 1979 to present.

b. Methodology to determine mechanisms of NAO-related precipitation variability

To determine the mechanisms of NAO-related precipitation anomalies we use a moisture budget approach. This was developed to analyze mechanisms of hydroclimate change (Seager et al. 2010b) and has been applied in the Mediterranean region (Seager et al. 2014) but can also be applied to studies of hydroclimate variability (Seager et al. 2012).

The moisture budget equation, assuming a steady state with no change in column integrated moisture over time, can be written in vertically discrete form as:

$$\overline{P} \approx \overline{E} - \frac{1}{g\rho_w}\nabla\cdot\sum_{k=1}^{K}\overline{\mathbf{u}}_k\,\overline{q}_k\overline{dp}_k - \frac{1}{g\rho_w}\nabla\cdot\sum_{k=1}^{K}\overline{\mathbf{u}_k' q_k'}\,\overline{dp}_k, \tag{1}$$

$$\approx \overline{E} - \frac{1}{g\rho_w}\sum_{k=1}^{K}\overline{\mathbf{u}}_k\cdot\nabla\overline{q}_k\overline{dp}_k - \frac{1}{g\rho_w}\sum_{k=1}^{K}\overline{q}_k\nabla\cdot\overline{\mathbf{u}}_k\overline{dp}_k$$

$$-\frac{1}{g\rho_w}\nabla\cdot\sum_{k=1}^{K}\overline{\mathbf{u}_k' q_k'}\,\overline{dp}_k - \frac{1}{g\rho_w}\overline{q_s\mathbf{u}_s\cdot\nabla p_s}. \tag{2}$$

Here P is precipitation, E is evaporation (taken to include transpiration), g is the acceleration due to gravity, ρ_w is the density of water, p is pressure, q is specific humidity and $\mathbf{u}$ the vector horizontal velocity. The overbar indicates monthly means and primes indicate departures of six-hourly values from monthly means. Subscript k indicates model level with pressure thickness dp_k. The second and third terms on the right of Eq. 1 are the moisture convergence by the mean flow

Accepted for publication in *Journal of Climate*. DOI 10.1175/JCLI-D-20-0011.1.

and submonthly transient eddies, respectively. The approximation in Eq. 1 comes from neglecting time rate of change of moisture (which is small for seasonal means compared to the other terms), ignoring terms involving dp'_k, errors introduced by using numerical methods distinct from those used in the ECMWF model, analysis increments and humidity tendencies in the model that were not archived and cannot be evaluated (e.g. diffusion; see Seager and Henderson (2013) for a discussion of all of these sources of error). In Eq. 2 the mean flow moisture convergence has been broken down into components due to moisture advection, i.e. flow across spatial gradients of moisture, and the divergent flow. The last term on the right hand side is a surface term that arises from bringing the divergence operator inside the vertical integral in order to enable the separation into advection and mass divergence terms. The computation of the vertical integrals, the horizontal divergences and the surface term are all done according to the "best practises" methodology of Seager and Henderson (2013) where these were developed using ERA-Interim data.

In Equations 1 and 2 all terms are first evaluated as monthly means and the seasonal means are evaluated by averaging over the monthly means. Seasonal anomalies of each term are computed as the departures of the seasonal means from the average across all years of the seasonal means. Here we only analyze the winter seasonal mean of December to March (DJFM).

We define the NAO as the first Empirical Orthogonal Function (EOF) of DJFM seasonal mean 500hPa heights in the European-Mediterranean-North Atlantic sector given by $60°W - 70°E$ and $0° - 90°N$. This region extends further east than is often used for NAO definitions but this is done to directly incorporate the Middle East within the region of study of NAO-precipitation relations. Typically a more longitudinally restricted range is used in the EOF analysis to define the NAO but this makes little difference to the retrieved NAO pattern. The EOF analysis is performed such that the spatial patterns carry the units (meters and mm/day) and the associated time series are in standardized units. The NAO-associated anomalies of P are evaluated by regressing DJFM

Accepted for publication in *Journal of Climate*. DOI 10.1175/JCLI-D-20-0011.1.

mean values of ERA-Interim P onto the time series associated with the first 500hPa height EOF. To understand the mechanisms of the P variability, the terms in the moisture budget equation are similarly regressed onto the time series. Significance of the P and moisture budget regressions is evaluated with a two sided t-test at the 5% level. To demonstrate the relevance of the NAO to regional precipitation variability we also conducted an EOF analysis of DJFM P for the same longitude domain but $15° - 90°N$ (to eliminate heavy tropical precipitation) and regressed 500hPa heights upon the time series of the leading mode.

To examine the dynamical underpinnings of transient eddy zonal and meridional moisture flux ($\overline{u'q'}$ and $\overline{v'q'}$) variability associated with the NAO we also examined the variability of $\overline{u'^2}$ and $\overline{v'^2}$ at 850hPa in the lower troposphere where moisture is concentrated. For a purer analysis of the associated storm track variability we analyzed variability of $\overline{v'^2}$ at 200hPa near where eddy kinetic energy of synoptic eddies maximizes.

The EOF and regression analyses focus on general associations and assume linearity. To assess whether these general relations can be used to explain precipitation anomalies in particular extreme winters we selected the two winters with the highest (1988/89) and lowest (2009/10) NAO values. We plot the P and moisture budget anomalies for these two winters as well as those reconstructed by multiplying the NAO-associated quantities by the NAO index for the two winters. To assess if the results for P from ERA-Interim are supported by direct observations the P anomalies from the CPC CMAP satellite-gauge data are plotted for the two extreme winters and time series of CPC CMAP precipitation and NAO values are plotted for the locations of four cities across the region (Glasgow, Bergen, Madrid, Belgrade). This work allows us to assess the mechanisms whereby extremes of the NAO translate into extremes of winter mean precipitation.

Accepted for publication in *Journal of Climate*. DOI10.1175/JCLI-D-20-0011.1.

3. Mechanisms of NAO-related precipitation variability

a. The circulation and precipitation anomalies of the NAO

Figure 1 in the left column shows the leading EOF of DJFM 500hPa height in the North Atlantic-Europe-Mediterranean region for both its spatial pattern (top row) and time series (bottom row, hereafter the NAO time series). As is well known, during its positive phase as shown, the NAO is associated with an anomalous low height anomaly extending from Hudson Bay to Scandinavia and centered around Iceland paired with a high height anomaly that extends from the southeast United States across the mid-latitude Atlantic Ocean and into continental Europe. The NAO has notable interannual variability and also trended downwards from the early 1990s to the end of the 2000s and has moved upward since. Figure 1 also shows the precipitation anomaly pattern found by regression on the NAO time series. There are wet anomalies over the subpolar North Atlantic, the northern British Isles and Scandinavia and dry anomalies over the eastern mid-latitude North Atlantic and southern Europe, in agreement with Trigo et al. (2004).

Figure 1 in the right column shows results from an EOF analysis of ERA-Interim P with regression of 500hPa heights on the associated time series (bottom row). This recovers the NAO patterns of circulation and precipitation making clear that this is the leading mode of winter season precipitation variability in this region. The middle row in Figure 1 shows the associated 850hPa wind vectors. In the high NAO phase westerly anomalies flow from the Labrador Sea to Scandinavia and easterly anomalies flow from Iberia to the Gulf of Mexico. The correlation coefficient of the time series from the EOF analyses of heights and precipitation is 0.94 which strongly emphasizes the dominance of the NAO on winter mean precipitation variability in the region.

Figure 2 shows the fraction of variance of seasonal mean precipitation explained by the NAO. For continental land areas in the Mediterranean this can vary up to 0.4. In Scotland and Scandi-

Accepted for publication in *Journal of Climate*. DOI 10.1175/JCLI-D-20-0011.1.

navia it can reach as high as 0.8 or above. In the southern British Isles and across Northern France, Germany and Poland the fraction is very small since these are aligned along a nodal line in the NAO-associated precipitation anomaly pattern. Over the subpolar eastern North Atlantic Ocean half of the variance of seasonal mean P is explained by the NAO.

b. Important aspects of the mean climate that the NAO perturbs

Figure 3 shows some key aspects of the mean climatology in the region that are essential to understanding how the circulation anomalies cause the P anomalies shown in Figure 1. The map of the climatological $\overline{v'^2}$ at 850hPa (upper left, contours) illustrates the storm track at levels in the troposphere where it can be effective in transporting moisture. A clear maximum extends northeastward from Nova Scotia to Norway. This storm activity occurs within an environment with a strong meridional gradient of vertically integrated moisture (upper left, shading) and, hence, will accomplish significant poleward moisture transport (lower left panel). The moisture transport maximizes on the southern edge of the storm track where the moisture gradient is stronger. The humidity field has a “ridge” that stretches from the Caribbean to Scotland and, consequently, the zonal transient eddy moisture flux (bottom right panel) is, in general, positive east and negative west of this ridge. The zonal eddy velocity variance (top right panel) exhibits less of a storm track structure but has a maximum between southern Greenland and Iceland, a region of strong zonal eddy drying. There is an exception to the general rule of down gradient eddy moisture transport east of the southeast US. Here the eddy moisture flux is eastward (Figure 3, bottom right) despite the mean vertically-integrated moisture increasing from west to east (Figure 3, top left). This is because of a strong positive covariance between zonal and upward eddy velocities (not shown), such that westerly anomalies are also upward and, hence, moist (an idea suggested by Prof. W.A. Robinson, pers. comm., May 2019). The climatological sea level pressure pattern

Accepted for publication in *Journal of Climate*. DOI 10.1175/JCLI-D-20-0011.1.

(upper right panel) emphasizes the strong southwest to northeast mean flow into the British Isles and Scandinavia between the Azores High and the Icelandic Low.

The NAO pattern (Figure 1) in combination with the climatological patterns (Figure 3) can be used to infer that the positive phase of the NAO will strengthen westerly flow from the Labrador Sea to Scandinavia, weaken the mid-latitude westerly flow around $30° - 40°N$ and strengthen the easterly trade wind flow from Iberia to the Gulf of Mexico. Considering how the NAO flow anomalies will interact with the mean humidity gradients, we expect the westerly and easterly wind anomalies to both induce advective drying over the subpolar and subtropical North Atlantic with the easterly wind anomalies inducing advective wetting over the mid-latitude ocean in between. However, other terms in the moisture budget will also come into play and need to be quantitatively determined.

c. The NAO-related moisture budget variability

Figure 4 shows the results of regressing P and the terms in the moisture budget in Eqs. 1 and 2 onto the time series associated with the first EOF of 500hPa heights (our defined NAO index). The P field is as in Figure 1. A striking feature to note is the extent to which over the ocean NAO-related anomalies in P are compensated for by anomalies in E. Over the subpolar (midlatitude) North Atlantic stronger (weaker) westerlies are associated with increased (decreased) E and P. It is reasonable to suppose that the changes in P result from the changes in E. Over the eastern North Atlantic the compensation between P and E is weaker with P winning the battle. As a consequence, the NAO-related $P-E$ anomaly is concentrated west of Iberia and north Africa and over the Norwegian Sea. There is a weaker dipole between negative $P-E$ in the Labrador Sea and positive $P-E$ east of the US and Canada in the western Atlantic basin. This pattern of $P-E$ anomalies, which is the freshwater forcing for the ocean, would favor enhanced salinity in the

Accepted for publication in *Journal of Climate*. DOI 10.1175/JCLI-D-20-0011.1.

Labrador Sea and reduced salinity in the Norwegian Sea and, in combination with SST changes, potentially, a shift of deep water formation from the latter to the former region (Zhang et al. 2019). However, salinity changes associated with the NAO are influenced by salt advection not just surface fluxes (Herbert and Houssais 2009).

The spatial patterns of NAO-associated $P-E$ anomalies (Figure 4c) closely match those of the mean flow moisture convergence (Figure 4d). Away from the Mediterranean and eastern Europe, the mean flow moisture convergence anomaly is dominated by the advection term (Figure 4f). However, the drying over the Mediterranean region for a positive NAO is associated with increased mean flow moisture and mass divergence, i.e. subsidence (Figure 4e). The surface term (Figure 4g) is noisy and clearly related to topography because of its inclusion of horizontal gradients of surface pressure, but we need not consider it more.

The transient eddy moisture convergence term (Figure 4h) to first order acts to simply oppose, but not fully offset, the $P-E$ anomaly pattern established by the mean flow moisture convergence anomaly. For example, during a positive NAO the transient eddy moisture convergence anomaly actually dries the British Isles and Scandinavia. Hence, despite the well remarked upon and dynamically active role that storm track variations play within NAO anomalies, the transient eddies play a primarily passive role and damp anomalies of $P-E$ generated by the mean flow circulation anomalies. To quantify this, the area-weighted spatial pattern correlation coefficient between the transient eddy (Figure 4h) and mean flow (Figure 4d) moisture flux convergences is -0.72. The transient eddy moisture flux convergence even more closely offsets the component of the mean flow moisture convergence that is due to advection (Figure 4f) with an area-weighted spatial pattern correlation coefficient of -0.77. Notably, the dry conditions over the Mediterranean during a positive NAO are not caused by reduced transient eddy moisture convergence in the Mediterranean stormtrack, with the exception of the east coast of Spain. In fact, over the eastern Mediterranean,

Accepted for publication in *Journal of Climate*. DOI 10.1175/JCLI-D-20-0011.1.

Greece and Turkey the transient eddy moisture convergence actually moistens and offsets mean flow moisture divergence due to subsidence during a positive NAO.

d. Dynamical interpretation of the NAO-associated precipitation variability

The key feature we wish to explain is the north-south dipole of increased-decreased P during a positive NAO that extends near zonally from the western North Atlantic well into Eurasia. First of all there is a role for evaporation anomalies. The NAO circulation anomaly with enhanced westerlies over the subpolar ocean and weakened westerlies over the midlatitude ocean generates a north-south dipole of enhanced-reduced E. The E anomalies arise from increased wind speed and increased dry advection over the subpolar ocean and reduced wind speed and reduced dry advection over the mid-latitude ocean (see Seager et al. (2000) for a quantitative decomposition of surface moist static energy fluxes).

NAO mean circulation anomalies also influence the advection and convergence of moisture. Over the western North Atlantic the westerly subpolar and southeasterly mid-latitude anomalies create dry and moist advection anomalies, respectively, that offset the E anomalies allowing for weak P anomalies. Over the eastern North Atlantic and Europe the westerly and moist advection anomaly to the north and easterly and dry advection anomaly to the south, in the presence of weak E anomalies, translate into positive P anomalies over the northern British Isles and Scandinavia and negative P anomalies over the subtropical eastern North Atlantic. The NAO-associated mass convergence anomaly dries most of Europe and is responsible for the Mediterranean region drying during a positive NAO. This is explained in terms of the NAO-associated northerly flow across most of Europe and the Mediterranean (Figure 1) which will induce, by cold advection and positive planetary vorticity advection, subsidence and low level mass divergence.

Accepted for publication in *Journal of Climate*. DOI 10.1175/JCLI-D-20-0011.1.

e. Understanding the role of transient eddies in the NAO-associated moisture budget variability

Next we seek to explain the role that transient eddy moisture fluxes, and NAO-associated changes in the strength and location of the stormtrack, play in generating anomalies of P. Figure 5a shows the familiar picture of NAO-associated storm track variability as seen in 250hPa $\overline{v'^2}$. For a positive NAO there is a clear northward shift and intensification of the storm track from North America well into Eurasia. The British Isles, Scandinavia and northern Europe see greater upper troposphere eddy activity and the Mediterranean region sees weaker activity. Within the lower troposphere the eddy activity anomalies look different, restricted to the eastern Atlantic and Eurasia region, and less coherent (Figure 5b). However, Scandinavia and Russia see an increase and some areas of the Mediterranean a decrease, in 850hPa $\overline{v'^2}$. For lower troposphere $\overline{u'^2}$ there is a broad decrease over the central North Atlantic (consistent with reduced blocking here during a positive NAO (Croci-Maspoli et al. 2007)) and an increase centered over the Norwegian Sea.

These changes in $\overline{v'^2}$ and $\overline{u'^2}$ acting on the unchanged humidity field would be expected to amplify or diminish the patterns of $\overline{v'q'}$ and $\overline{u'q'}$ (Figure 3). This is the case for $\overline{v'q'}$ over Scandinavia and the southwestern Europe-eastern mid-latitude Atlantic region where increases and decreases, respectively, co-locate with increased and decreased $\overline{v'^2}$. The pattern of change in $\overline{u'q'}$ can also partly be explained by the pattern of change in $\overline{u'^2}$. In the Labrador Sea and east of Newfoundland reduced $\overline{u'^2}$ leads to weakening the negative $\overline{u'q'}$ that prevails there. Reduced $\overline{u'q'}$ over Iberia and to its southwest can also be explained in terms of reduced $\overline{u'^2}$.

The anomalies of $\overline{u'q'}$ and $\overline{v'q'}$ can also be influenced by changes in the humidity field gradients (Figure 5d) driven by the NAO mean circulation anomalies. The anomalous zonal gradients are weak and do not strongly influence $\overline{u'q'}$ except over Russia where this term moistens eastward of the humidity increase over the Baltic Sea. The meridional gradients of humidity anomalies are, in

Accepted for publication in *Journal of Climate*. DOI 10.1175/JCLI-D-20-0011.1.

contrast, strong and the meridional transient eddy moisture flux anomalies, $\overline{v'q'}$, are well explained in terms of a down-gradient transport of moisture anomalies. The southwest to northeast band of northward transient eddy moisture transport between the northeast US and Scandinavia (Figure 3, lower left) removes moisture from the similarly oriented band of anomalously high moisture between Florida and northwest Europe and into the area of anomalously low moisture over the Labrador Sea, Greenland and the Greenland Sea (Figure 5d). The strong southward transient eddy moisture transport (which is really reduced northward transport) stretching southwest from Iberia and the Bay of Biscay moves less moisture from the region of anomalously low moisture extending southwest from Iberia to the region of anomalously high moisture to its north.

The NAO-associated moisture anomaly can be understood in terms of the mean flow anomalies. The drier regions over the northwest and southeast North Atlantic (Figure 5d) occur where the flow anomaly induces dry advection from dry continental regions or cooler waters (Figure 4f). The band of moist anomalies in between (Figure 5d) occurs where the mean flow anomaly is westerly (Figure 1, middle row) and from moist regions above the North Atlantic Drift and Norwegian Current to drier regions eastward and over land (the British Isles and Scandinavia) and where there is a southerly component to the flow anomaly (east of the United States, Figure 1, middle row). The transient eddy moisture fluxes then work to oppose these anomalies generated by the mean flow (Figure 4h).

Consequently, transient eddies work to remove humidity anomalies created by the NAO, but also play an active role by altering moisture fluxes where the storm tracks weaken and strengthen.

4. The NAO and extreme wet and dry winters in the Europe-Mediterranean region

The work presented so far concerns the general relation between the NAO and precipitation variations and the physical mechanisms involved. But, as Figure 2 makes clear, while the NAO is

Accepted for publication in *Journal of Climate*. DOI 10.1175/JCLI-D-20-0011.1.

the dominant mode of variability of winter season precipitation in the region, it does not explain everything. Hence next we consider how well the NAO correlates with precipitation variability in specific locations across the region and then examine spatial patterns of precipitation and moisture budget anomalies for the two winters with the most positive and negative NAO anomalies.

Figure 6 shows time series of concurrent seasonal NAO and CPC CMAP precipitation anomalies for grid point locations nearest to Glasgow, Bergen, Madrid and Belgrade. The results are consistent with the maps of NAO-explained precipitation variance in Figure 2 and show strong positive correlations in Glasgow and Bergen and a slightly weaker negative correlation in Madrid. The negative correlation in Belgrade is much weaker, consistent with the weakening of the NAO-explained variance eastward across the Mediterranean region. At Glasgow, Bergen and Madrid most of the precipitation maxima and minima occurred together with NAO extremes but each location had some exceptions: 2002/3 was very dry in Glasgow and 2004/5 was very wet in Bergen but both winters were NAO neutral, while 1981/2 was wet in Madrid even though the NAO was positive. [1] The most positive NAO winter was 1988/9 and the most negative NAO winter was 2009/10. Figure 6 shows the NOAA CPC CMAP precipitation anomalies for these winters. Values are shown only over land where the data are constrained by rain gauges and the CPC CMAP data are used as a robustness check on the more reanalysis model-dependent ERA-Interim values analyzed next. Both winters had distinctive NAO precipitation anomalies with, in 1988/89, wet over the northern British Isles and Scandinavia and dry across Iberia, southern France and all countries north of the Mediterranean Sea as well as northwest Africa. In 2009/10 the precipitation anomaly pattern

[1] Investigation of these non-NAO related extreme winter precipitation anomalies (not shown) reveals: the dry winter of 2002/3 in Glasgow was related to a high anomaly centered over the Norwegian Sea that brought easterly anomalies (i.e. opposed moist westerlies) to Scotland; the wet winter of 2004/5 in Bergen was related to a high anomaly centered approximately equidistant between Newfoundland and Iceland that brought northwesterlies off the Norwegian Sea to Bergen; the wet winter of 1981/2 in Madrid was related to a very deep low centered over Denmark that brought strong westerly anomalies from the Atlantic Ocean over Iberia and this was overwhelmingly dominated by December 1981.

Accepted for publication in *Journal of Climate*. DOI 10.1175/JCLI-D-20-0011.1.

was approximately reversed. The nodal line between positive and negative anomalies was notably located more south in the negative NAO winter than in the positive NAO winter.

How well can the precipitation anomalies in these two NAO-extreme winters be accounted for by just the NAO and what are the mechanisms for their generation? The NAO contribution to precipitation for each winter can be derived by multiplying the EOF spatial pattern in Figure 1 (top left) with the associated time series value for the winter. The NAO contributions for other terms can be derived similarly from spatial regressions on the NAO index and the NAO values for the winters. For the extreme positive NAO winter of 1988/9 the NAO well explains the anomaly patterns of P, E and $P-E$ (Figure 7) with area-weighted spatial pattern correlation coefficients of 0.77, 0.83 and 0.70 respectively. The concentration of large $P-E$ anomalies in the eastern part of the region, due to cancellation of P and E over the western Atlantic that was seen in the general relations, also occurs in this winter too. The contributions to $P-E$ of the mean flow and transient eddy moisture flux convergence anomalies are also well accounted for by their NAO-associated components (Figure 8) with area-weighted spatial pattern correlation coefficients of 0.66 and 0.57 respectively. The mean flow moisture convergence drives the wetting in the northern British Isles and Scandinavia and the drying across the Mediterranean region. Transient eddies offset the wetting in northern Europe.

Winter 2009/10 is famous for its extreme cold in northern Europe, attributed to the extremely negative NAO (Seager et al. 2010a; Cohen et al. 2010; Cattiaux et al. 2010) which itself was likely influenced by the 2009/10 El Niño and an easterly Quasi-Biennial Oscillation phase (Fereday et al. 2012). Although less remarked upon, it was also a winter with strong negative precipitation anomalies across the northern British Isles and Scandinavia and strong wet anomalies across Iberia, Morocco and the countries along the north shores of the Mediterranean Sea (Figures 6 and 9). The P, E and $P-E$ anomalies are well accounted for by the NAO contribution with area-

Accepted for publication in *Journal of Climate*. DOI 10.1175/JCLI-D-20-0011.1.

weighted spatial pattern correlation coefficients of 0.81, 0.78 and 0.77 respectively. As for the extreme positive NAO winter, the $P-E$ anomalies are concentrated in the east where the P and E anomalies do not offset each other. Also as for the positive NAO winter and the general case, the dry and wet anomalies in the northern British Isles and Scandinavia and the Mediterranean region, respectively, were generated by the mean flow moisture convergence and, in the former case, offset by the transient eddy moisture fluxes (Figure 10). The NAO contribution largely accounts for these moisture budget anomalies with area-weighted spatial pattern correlation coefficients of 0.76 and 0.69 for the mean and transient components (Figure 10).

5. Conclusions

We have presented an observations-based analysis of the physical mechanisms of winter seasonal mean precipitation variability associated with the NAO. The work was based on analyses of interannual circulation and precipitation variability and associated moisture budget variability within the ERA-Interim Reanalysis for 1979 to 2017. To our knowledge this provides the most detailed analysis to date of how mean and transient circulation anomalies associated with the NAO translate into precipitation anomalies that have significant social impacts on water resources, power generation, streamflows and agriculture across the Europe and Mediterranean region. Our conclusions are as follows.

- The NAO is the leading mode of winter seasonal mean circulation variability in the Atlantic-Europe-Mediterranean region. The leading mode of winter seasonal mean precipitation variability is clearly associated with the NAO. NAO-related precipitation variability accounts for 50% or more of seasonal precipitation variability in the northern British Isles and Scandinavia and 20-50% in Morocco and the countries along the north shore of the Mediterranean Sea.

Accepted for publication in *Journal of Climate*. DOI 10.1175/JCLI-D-20-0011.1.

- The precipitation anomalies associated with the NAO are primarily driven by the mean flow moisture convergence anomalies. The precipitation anomalies are to a lesser extent influenced by the NAO-related shifts in the storm tracks and the associated anomalies in the transient eddy moisture fluxes. Transient eddy moisture fluxes largely act diffusively to oppose the changes in precipitation created by the mean flow anomalies and notably offset the mean flow moisture convergence-driven precipitation anomalies over the British Isles and Scandinavia.
- Precipitation anomalies over the northern British Isles and Scandinavia are primarily driven by anomalies in moisture advection related to anomalies in the prevailing southwesterly flow with the transient eddy moisture fluxes opposing the mean-flow induced changes in precipitation. Over continental Europe and the Mediterranean region the precipitation anomalies are instead driven by changes in the mean flow moisture convergence related to anomalies in low level mass convergence and subsidence.
- The precipitation variability over the Mediterranean region is driven by the mean flow anomalies and not strongly influenced by the transient eddies in the local storm track even though there is a noticeable weakening of the strength of the transient eddies in the lower troposphere during a positive NAO. However, during a positive NAO, transient eddy moisture flux convergence notably offsets drying by the mean flow moisture convergence.
- These general relations hold true for extreme winters. The two most extreme NAO winters are also winters of extreme precipitation anomalies across the British Isles and Scandinavia and the Mediterranean. NAO-associated mean flow moisture convergence anomalies are the causal mechanisms for these extreme seasonal precipitation events.

This diagnostic work allows a conceptual model of how the NAO generates precipitation variations to be developed which we illustrate for the case of a positive NAO. A positive NAO establishes low

Accepted for publication in *Journal of Climate*. DOI 10.1175/JCLI-D-20-0011.1.

level southwesterly flow from the eastern US to Scandinavia, northerly flow over southern continental Europe and easterly flow over the subtropical Atlantic. Via enhanced (reduced) wind speed and dry advection this creates enhanced (reduced) evaporation over the subpolar (subtropical) North Atlantic Ocean. Over the western Atlantic Ocean the changes in advection and evaporation largely balance. Further east where the changes in evaporation are smaller, precipitation increases where the flow is southwesterly and decreases where it is northerly or easterly, due to enhanced (reduced) mean flow moisture convergence. Increased precipitation occurs over the northern and western British Isles and Scandinavia as the enhanced southwesterlies meet topography. Reduced precipitation occurs over southern continental Europe and the Mediterranean region under the influence of subsiding air and mean flow moisture divergence. The mean flow anomalies also create, via dry advection, regions of reduced column-integrated moisture over the subpolar and subtropical North Atlantic with a region of enhanced moisture caused by moist advection in between. Transient eddy moisture fluxes primarily work to damp these humidity anomalies. In addition, the poleward shift of the storm track in the lower atmosphere creates a transient eddy moisture divergence anomaly that partly offsets the increase in precipitation driven by the mean flow anomalies over the northern British Isles and Scandinavia.

It is worth noting that the patterns and mechanisms of NAO-related moisture budget variability are distinctly different from those related to greenhouse gas-driven climate change. Radiatively-forced hydroclimate change in the Mediterranean region has been examined by Seager et al. (2014). The NAO-related $P-E$ pattern has a quadrople structure with strongest anomalies over Europe and the Mediterranean region. In contrast, the modeled and observed climate change pattern of $P-E$ change is much more zonally uniform (see Seager et al. (2019) for a comparison of these). The essential mechanism difference is that under greenhouse gas-induced change the atmospheric temperature and specific humidity increase everywhere. This creates a strong ther-

Accepted for publication in *Journal of Climate*. DOI 10.1175/JCLI-D-20-0011.1.

modynamic component to hydroclimate change. This works to amplify the existing pattern of $P-E$ as moisture convergence increases in ascending regions and moisture divergence increases in descending regions. In addition, transient eddy moisture transports also increase which again dries subtropical regions and moistens higher latitudes, especially over eastern North America and the North Atlantic. However, the dynamical components related to changes in mass convergence are similar between the NAO and climate change. For both climate change and a positive NAO, descent over southern Europe and the Mediterranean region causes reduced $P-E$ but ascent over some regions of northwest Europe causes increased $P-E$. Despite some commonalities, even these dynamical patterns are different because the climate change induced circulation change is distinct from that of the NAO. This makes clear that future hydroclimate change in the European-Mediterranean cannot be explained using an NAO analogy.

The work suggests some clear directions for future research. Given the strong influence of the NAO on European and Mediterranean winter climate, skillful predictions and projections of regional weather, climate variability and climate change requires skilful prediction of the NAO-associated components. Hence it is important to assess not just how well models simulate the NAO as a circulation phenomenon but also how well they simulate the mechanisms of NAO-associated precipitation variability. In particular, it needs to be assessed whether models have the correct spatial patterns and amplitudes of the mean flow and transient eddy moisture convergence and evaporation/evapotranspiration contributions to NAO-associated precipitation variability. Biases in this regard will translate into biases in the NAO-related precipitation variability but, having been diagnosed, will identify where efforts at model improvement must be directed. The conclusions presented here regarding transient eddies could also be checked using methods that use storm tracking and attribute precipitation to storms, as Zappa et al. (2015) have done in the climate change context. Of particular interest will be to examine how, in environments where precipitation

Accepted for publication in *Journal of Climate*. DOI 10.1175/JCLI-D-20-0011.1.

often occurs within storms (e.g. the Mediterranean), the mean flow interacts with the storms such that the precipitation variability is accounted for by the mean flow moisture convergence variability.

Acknowledgments. The research at Lamont Doherty Earth Observatory was supported by NSF award AGS-1734760. IRS is supported by the National Center for Atmospheric Research, which is a major facility sponsored by the National Science Foundation under the Cooperative Agreement 1852977. We thank Naomi Henderson for her essential work with the ERA-Interim Reanalysis and moisture budget decomposition, Walter Robinson for useful discussions and three reviewers for constructive critiques.

References

Anderson, W., R. Seager, W. Baethgen, and M. Cane, 2019: Synchronous crop failures and climate-forced production variability. *Sci. Adv.*, **5**, DOI:10.1126/sciadv.aaw1976.

Baldwin, M., and T. Dunkerton, 2001: Stratospheric harbingers of anomalous weather regimes. *Science*, **294**, 581–584.

Barnes, E. A., and D. L. Hartmann, 2010: Dynamical feedbacks and the persistence of the NAO. *J. Atmos. Sci.*, **67**, 851–865.

Cattiaux, J., R. Vautard, C. Cassou, P. Yiou, V. Masson-Delmonte, and F. Codron, 2010: Winter 2010 in Europe: A cold event in a warming climate. *Geophys. Res. Lett.*, **37**, doi:10.1029/2010GL044 613.

Cherry, J., H. Cullen, M. Visbeck, A. Small, and C. Uvo, 2005: Impacts of the North Atlantic Oscillation on Scandinavian hydropower production and energy markets. *Water Resources Management*, **19**, 673–691.

Accepted for publication in *Journal of Climate*. DOI 10.1175/JCLI-D-20-0011.1.

Cohen, J., J. Foster, M. Barlow, K. Saito, and J. Jones, 2010: Winter 2009-2010: A case study of an extreme Arctic Oscillation event. *Geophys. Res. Lett.*, **37**, L17 707,doi:10.1029/2010GL044 256.

Cook, E., Y. Kushnir, J. E. Smerdon, A. P. Williams, K. Anchukaitis, and E. Wahl, 2019: A Euro-Mediterranean tree-ring reconstruction of the winter NAO indices since 910 C.E. *Clim. Dyn.*, **53**, 1567–1580, doi.org/10.1007/s00 382–019–04 696–2.

Croci-Maspoli, M., C. Schwarz, and H. Davies, 2007: Atmospheric blocking: space-time links to the NAO and PNA. *Clim. Dyn.*, **29**, 713–725.

Cullen, H. M., A. Kaplan, P. A. Arkin, and P. B. deMenocal, 2002: Impact of the North Atlantic Influence on Middle Eastern climate and streamflow. *Climatic Change*, **55**, 315–338.

DeWeaver, E., and S. Nigam, 2000: Zonal-eddy dynamics of the North Atlantic Oscillation. *J. Climate*, **13**, 3893–3914.

Feldstein, S., 2000: The timescale, power spectra, and climate noise properties of teleconnection patterns. *J. Climate*, **13**, 4430–4440.

Feldstein, S., 2002: The recent trend and variance increase of the annular mode. *J. Climate*, **15**, 88–94.

Fereday, D., A. Maidens, A. A. abd A.A. Scaife, and J. R. Kinight, 2012: Seasonal forecasts of northern hemipshere winter 2009/10. *Env. Res. Lett.*, **7**, 034 031.

Herbert, C., and M. Houssais, 2009: Response of the eastern North Atlantic subpolar gyre to the North Atlantic Oscillation. *Geophys. Res. Lett.*, **36**, L17 607,soi:10.1029/2009GL039 090.

Hurrell, J. W., 1995: Decadal trends in the North Atlantic Oscillation: Regional temperatures and precipitation. *Science*, **269**, 676–679.

Accepted for publication in *Journal of Climate*. DOI 10.1175/JCLI-D-20-0011.1.

Ineson, S., and A. A. Scaife, 2009: The role of the stratosphere in the european climate response to el niño. *Nature Geosci.*, **2**, 32–36.

Jerez, S., R. M. Trigo, S. M. Vicente-Serrano, D. Pozo-Vazquez, R. Lorente-Plaza, J. Lorenzo-Lacruz, F. Santos-Alamillos, and J. Montavez, 2013: The impact of the North Atlantic Oscillation on renewable energy resources in southwestern Europe. *J. Appl. Meteor. Clim.*, 2204–2225.

Kidston, J., A. A. Scaife, S. Hardiman, D. M. Mitchell, N. Butchart, M. P. Baldwin, and L. J. Grey, 2015: Stratospheric influence on tropospheric jet streams, storm tracks and surface weather. *Nature Geo.*, **8**, 433–440.

Kim, W. M., S. Yeager, P. Chang, and G. Danabasoglu, 2018: Low-frequency North Atlantic climate variability in the Community Earth System Model large ensemble. *J. Climate*, **31**, 787–813.

Kravtsov, S., 2017: Pronounced differences between observed and CMIP5-simulated multi-decadal climate variability in the twentieth century. *Geophys. Res. Lett.*, **44**, 5794–5757, doi:10.1002/2017GL074 016.

Krichak, S. O., J. S. Breitgand, S. Gualdi, and S. B. Feldstein, 2014: Teleconnection-extreme precipitation relationships over the Mediterranean region. *Theor. Appl. Climatol.*, **117**, 679–692.

Mellado-Cano, J., D. Barriopedro, R. Garcia-Herrera, R. M. Trigo, and A. Hernandez, 2019: Examining the North Atlantic Oscillation, East Atlantic pattern and jet stream variability since 1685. *J. Climate*, **32**, 6285–6298.

Osborn, T. J., 2004: Simulating the winter North Atlantic Oscillation: The roles of internal variability and greenhouse gas forcing. *Clim. Dyn.*, **22**, 605–623.

Accepted for publication in *Journal of Climate*. DOI 10.1175/JCLI-D-20-0011.1.

Osborn, T. J., 2011: Variability and changes in the North Atlantic Oscillation index. *Hydrological, Socioeconomic and Ecological Impacts of the North Atlantic Oscillation in the Mediterranean Region*, S. Vicente-Serrano, and R. Trigo, Eds., Springer, Dordrecht, 9–22.

Pinto, J. G., and C. C. Raible, 2012: Past and recent changes in the North Atlantic Oscillation. *WIREs Clim. Change*, **3**, 79–90.

Rogers, J., 1997: North Atlantic storm track variability and its association to the North Atlantic Oscillation and climate variability of Northern Europe. *J. Climate*, **10**, 1635–1645.

Scaife, A., and Coauthors, 2014: Skillful long-range predictions of European and North American winters. *Geophys. Res. Lett.*, **41**, doi10.1029/2014GL059 637.

Seager, R., and N. Henderson, 2013: Diagnostic computation of moisture budgets in the ERA-Interim Reanalysis with reference to analysis of CMIP-archived atmospheric model data. *J. Climate*, **26**, 7876–7901.

Seager, R., Y. Kushnir, M. Ting, N. Naik, and J. Nakamura, 2010a: Northern hemisphere winter snow anomalies: ENSO, NAO and the winter of 2009/10. *Geophys. Res. Lett.*, **37**, doi:10.1029/2010GL043 830.

Seager, R., Y. Kushnir, M. Visbeck, N. Naik, J. Miller, G. Krahmann, and H. Cullen, 2000: Causes of Atlantic Ocean climate variability between 1958 and 1998. *J. Climate*, **13**, 2845–2862.

Seager, R., H. Liu, N. Henderson, I. Simpson, C. Kelley, T. Shaw, Y. Kushnir, and M. Ting, 2014: Causes of increasing aridification of the Mediterranean region in response to rising greenhouse gases. *J. Climate*, **27**, 4655–4676.

Accepted for publication in *Journal of Climate*. DOI 10.1175/JCLI-D-20-0011.1.

Seager, R., N. Naik, and G. A. Vecchi, 2010b: Thermodynamic and dynamic mechanisms for large-scale changes in the hydrological cycle in response to global warming. *J. Climate*, **23**, 4651–4668.

Seager, R., N. Naik, and L. Vogel, 2012: Does global warming cause intensified interannual hydroclimate variability? *J. Climate*, **25**, 3355–3372.

Seager, R., T. J. Osborn, Y. Kushnir, I. R. Simpson, J. Nakamura, and H. Liu, 2019: Climate variability and change of Mediterranean-type climates. *J. Climate*, **32**, 2887–2915.

Shindell, D. T., R. L. Miller, G. A. Schmidt, and L. Pandolfo, 1999: Greenhouse gas forcing of Northern Hemisphere winter climate trends. *Nature*, **399**, 452–455.

Simpson, I., C. Deser, K. McKinnon, and E. Barnes, 2018: Modeled and observed multidecadal variability in the North Atlantic jet stream and its connection to sea surface temperatures. *J. Climate*, **31**, 8313–8338.

Trigo, I. F., D. Pozo-Vazquez, T. J. Osborn, Y. Castro-Diez, S. Gamiz-Fortis, and M. J. Esteban-Parra, 2004: North Atlantic Oscillation influence on precipitation, river flow and water resources in the Iberian peninsula. *Int. J. Climatol.*, **24**, 925–944.

van Loon, H., and J. C. Rogers, 1978: The seesaw in winter temperatures between Greenland and Northern Europe. Part I: General description. *Mon. Wea. Rev.*, **106**, 296–310.

Walker, G., and E. Bliss, 1932: World Weather V. *Mem. R. Meteorol. Soc.*, **4 (36)**, 53–84.

Wang, X., J. Li, C. Sun, and T. Liu, 2017: NAO and its relationship with the Northern Hemisphere surface temperature in CMIP5 simulations. *J. Geophys. Res.-Atmos.*, **122**, 4202–4227, doi:10.1002/2016JD025 979.

Accepted for publication in *Journal of Climate*. DOI 10.1175/JCLI-D-20-0011.1.

Xie, P., and P. A. Arkin, 1996: Analyses of global monthly precipitation using gauge observations, satellite estimates, and numerical model predictions. *J. Climate*, **9**, 840–858.

Xie, P., and P. A. Arkin, 1997: Global precipitation: A 17-year monthly analysis based on gauge observations, satellite estimates, and numerical model outputs. *Bull. Amer. Meteor. Soc.*, **78**, 2539–2558.

Zappa, G., M. K. Hawcroft, L. C. Shaffrey, E. Black, and D. J. Brayshaw, 2015: Extratropical cyclones and the projected decline of winter Mediterranean precipitation in the CMIP5 models. *Clim. Dyn.*, **45**, 1727–1738, doi:10.1007/s00 382–014–2426–8.

Zhang, R., R. Sutton, G. Danabasoglu, Y. Kwon, R. Marsh, S. G. Yeager, D. E. Amrhein, and C. M. Little, 2019: A review of the role of the Atlantic Meridional overturning circulation in Atlantic multidecadal variability and associated climate impacts. *Rev. Geophys.*, **57**, 316–375 doi.org/10.1029/2019RG000 644.

Accepted for publication in *Journal of Climate*. DOI 10.1175/JCLI-D-20-0011.1.

LIST OF FIGURES

Accepted for publication in *Journal of Climate*. DOI 10.1175/JCLI-D-20-0011.1.

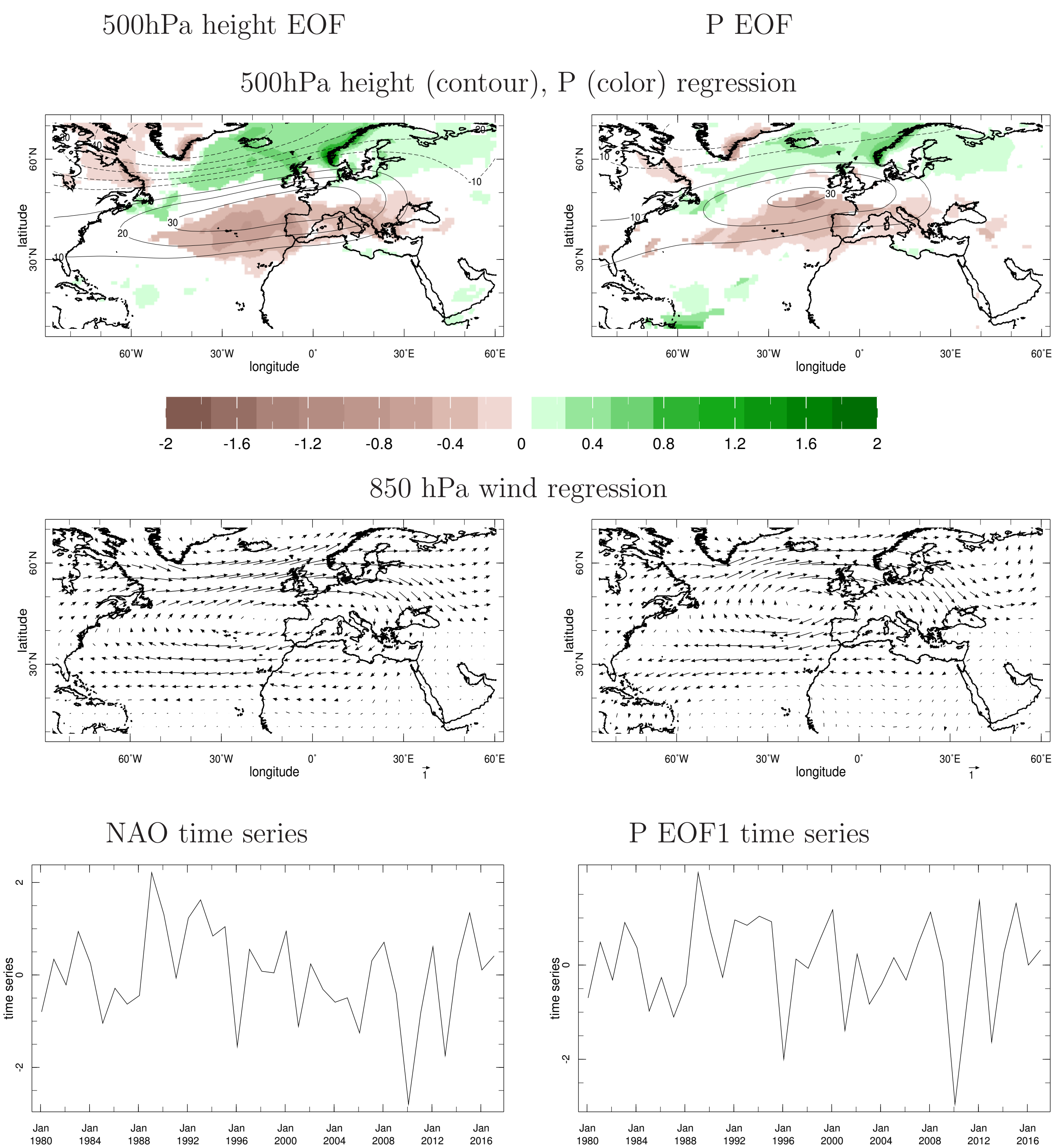

FIG. 1. Patterns of winter (DJFM) 500hPa height (contours) and precipitation (colors) obtained for (top left) an EOF analysis of 500hPa heights and (top right) an EOF analysis of precipitation and regression on the associated time series (bottom row), based on ERA-Interim data (the marked year refers to the January of the winter mean). The middle row shows the regressions of the 850hPa wind vectors. Units are hPa, m/s and mm/month per standard deviation of the time series. The correlation coefficient between the time series is 0.94.

Accepted for publication in *Journal of Climate*. DOI 10.1175/JCLI-D-20-0011.1.

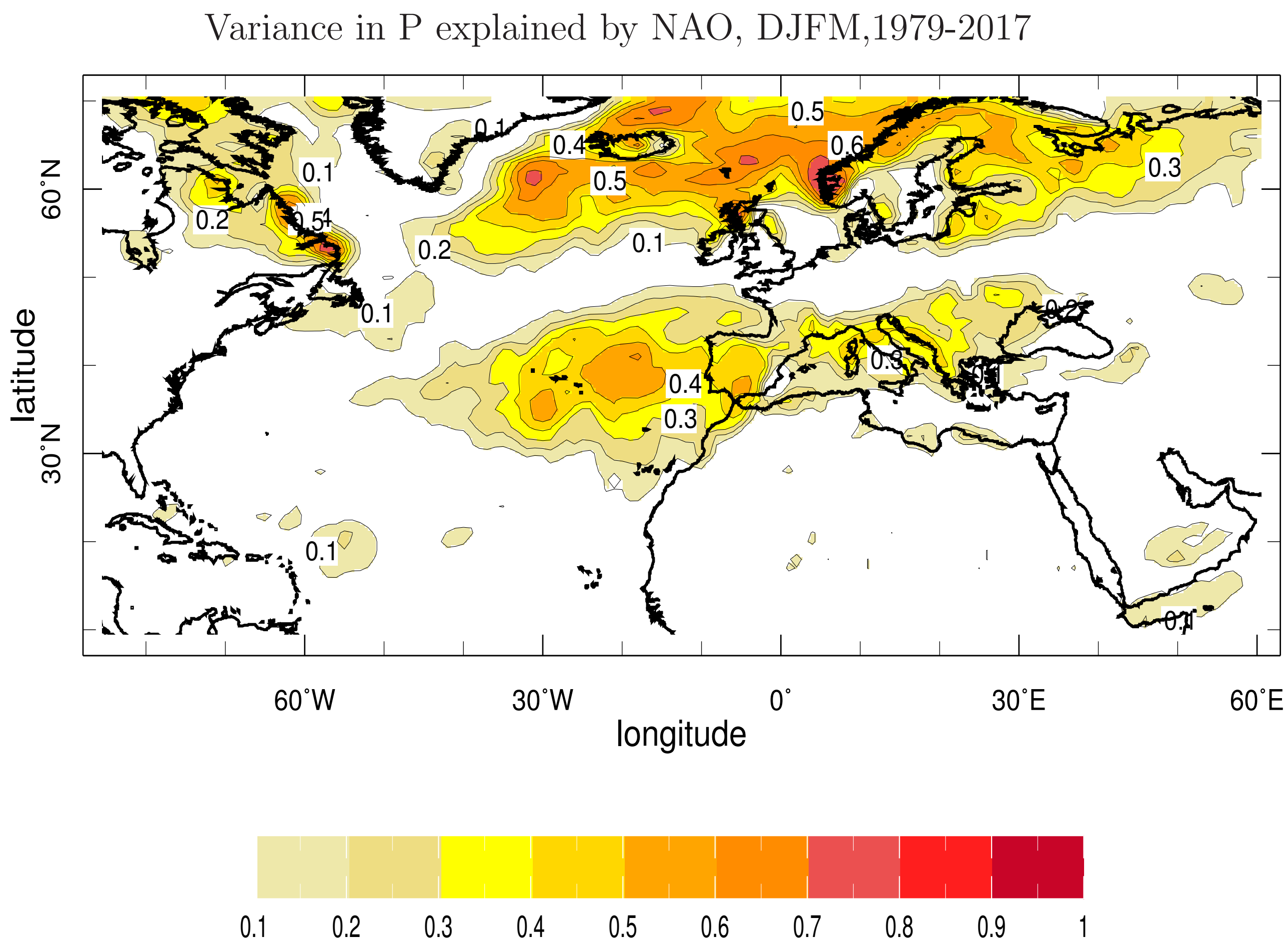

FIG. 2. The fraction of variance in winter precipitation explained by the NAO, based on ERA-Interim data.

Accepted for publication in *Journal of Climate*. DOI 10.1175/JCLI-D-20-0011.1.

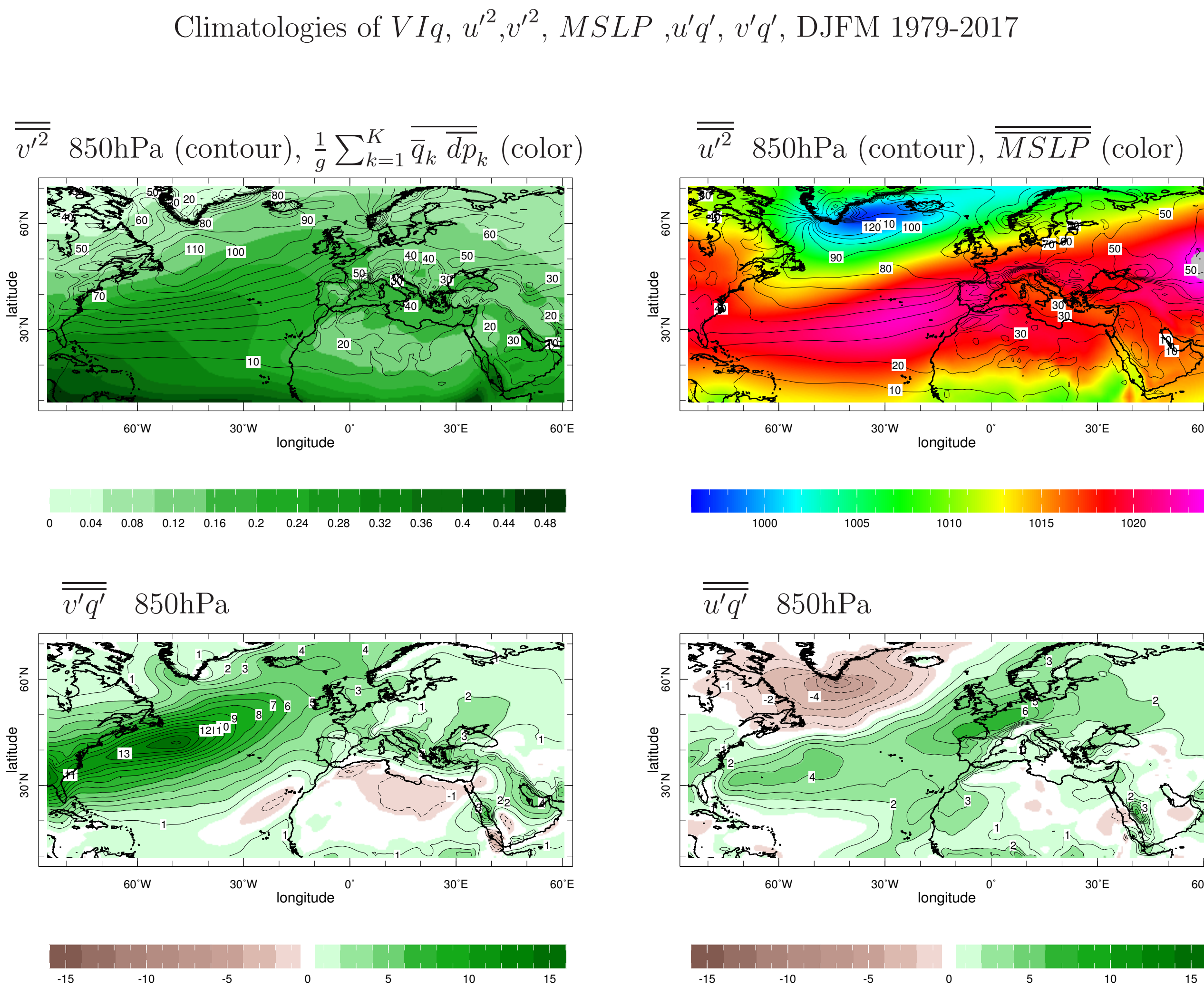

FIG. 3. Climatologies of quantities important to winter precipitation variability in the Atlantic-European-Mediterranean domain. Top left shows the vertically integrated humidity in colors (kg/m^2) and 850mb transient eddy meridional velocity variance in contours (m^2/s^2). Upper right shows the mean sea level pressure in colors (hPa) and the transient eddy zonal velocity variance (m^2/s^2). Lower left and right shows the climatological transient eddy meridional and zonal moisture flux at 850hPa (m/s) times 1000.

Accepted for publication in *Journal of Climate*. DOI 10.1175/JCLI-D-20-0011.1.

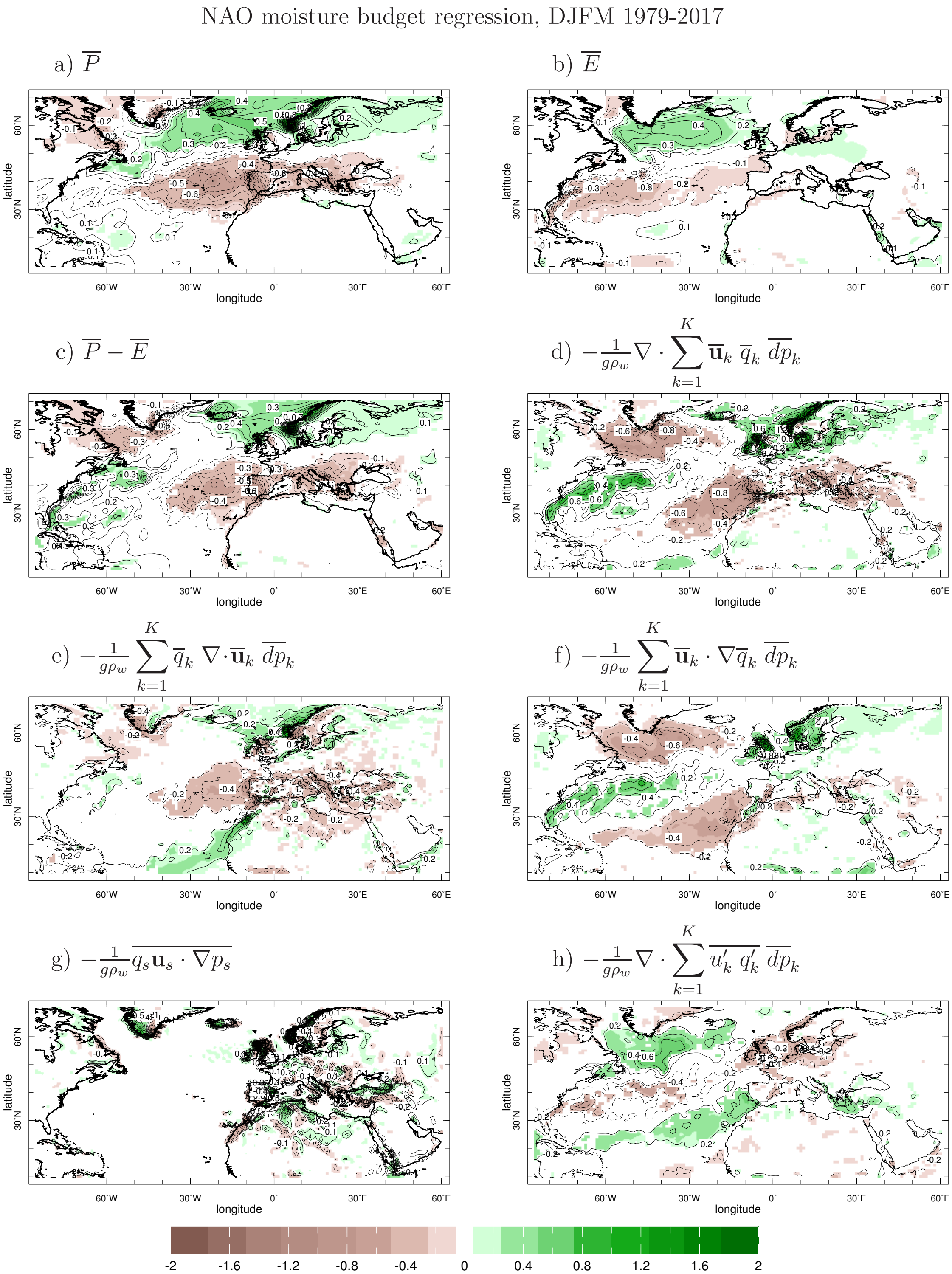

FIG. 4. Terms in the moisture budget regressed onto the NAO index for a) P, b) E, c) $P-E$, d) convergence of vertically integrated mean flow moisture flux, and the components related to e) mass convergence, f) moisture advection and, g) the surface term and h) the convergence of vertically integrated transient eddy moisture flux. Color shading is added where the anomalies are significant at the 95% level according to a two tail t-test. All are in units of mm/day.

Accepted for publication in *Journal of Climate*. DOI 10.1175/JCLI-D-20-0011.1.

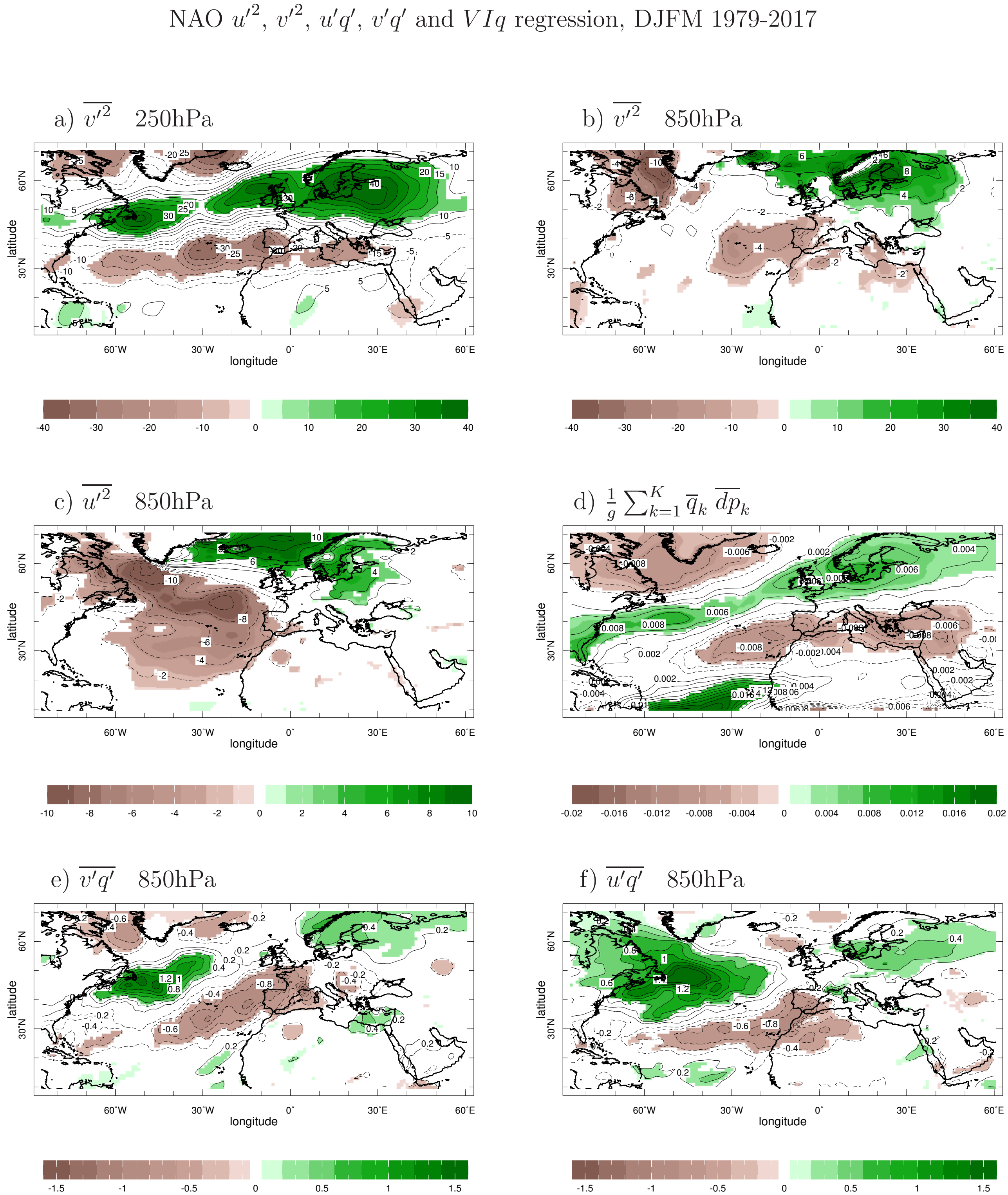

669 FIG. 5. Regression on the NAO index of a) $\overline{v'^2}$ at 250hPa (m^2/s^2), b) $\overline{v'^2}$ at 850hPa (m^2/s^2), c) $\overline{u'^2}$ at 850hPa
670 (m^2/s^2), d) vertically integrated specific humidity (kg/m^2) and transient eddy moisture fluxes at 850hPa in the
671 e) meridional and f) zonal direction ($kg(m/s)$). Color shading is added where the anomalies are significant at
672 the 95% level according to a two-sided t-test.

Accepted for publication in *Journal of Climate*. DOI 10.1175/JCLI-D-20-0011.1.

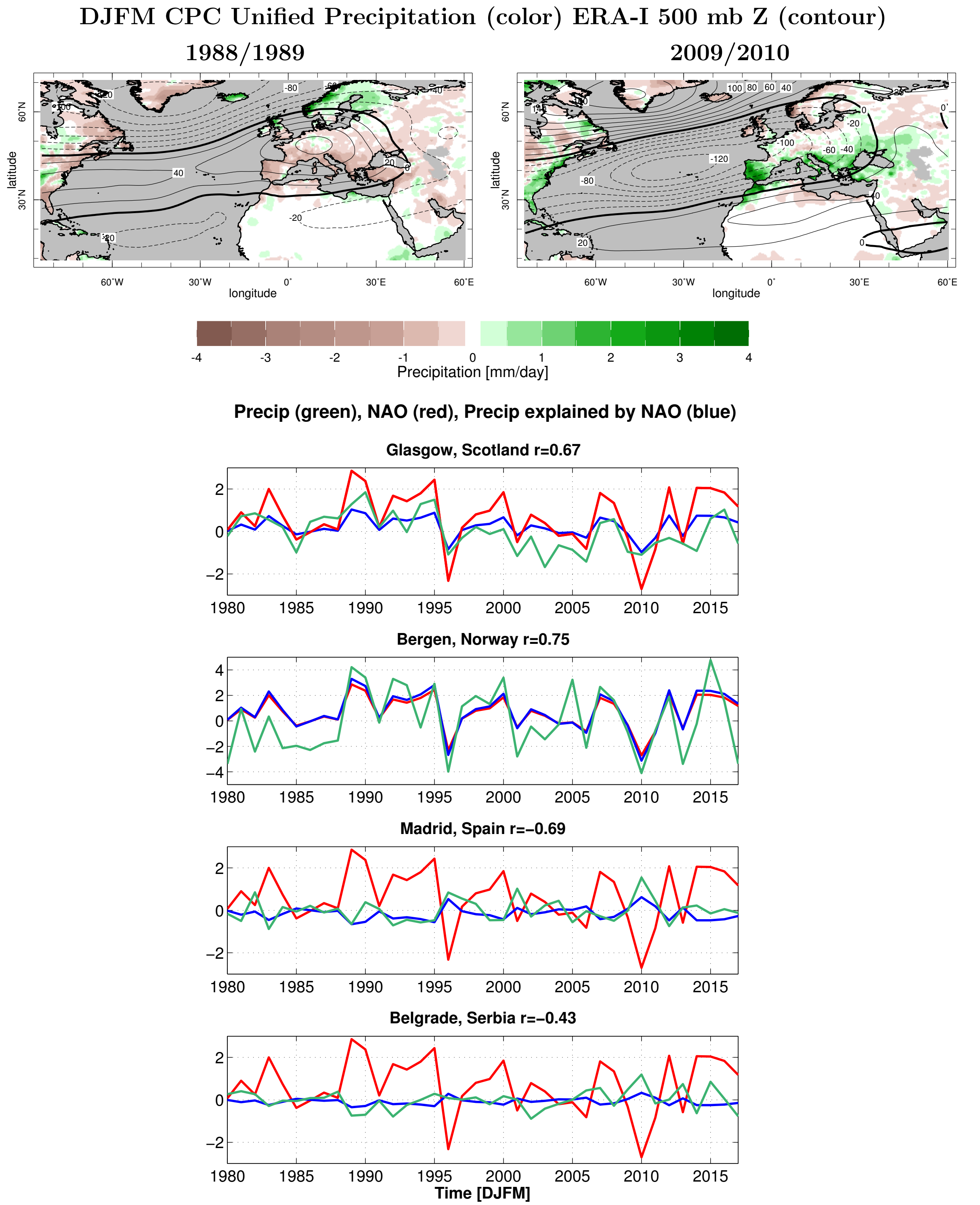

FIG. 6. The observed satellite-gauge precipitation anomaly over land (colors) and 500hPa height (contours) for the most extreme positive (top left) and negative (top right) winters since 1979. Units are mm/day and meters. The four panels below show the NAO index, the observed precipitation, and that accounted for by the NAO, for Glasgow, Bergen, Madrid and Belgrade together with the correlation coefficients between the NAO and observed precipitation. The NAO is in standardized units and the precipitation in mm/day.

Accepted for publication in *Journal of Climate*. DOI 10.1175/JCLI-D-20-0011.1.

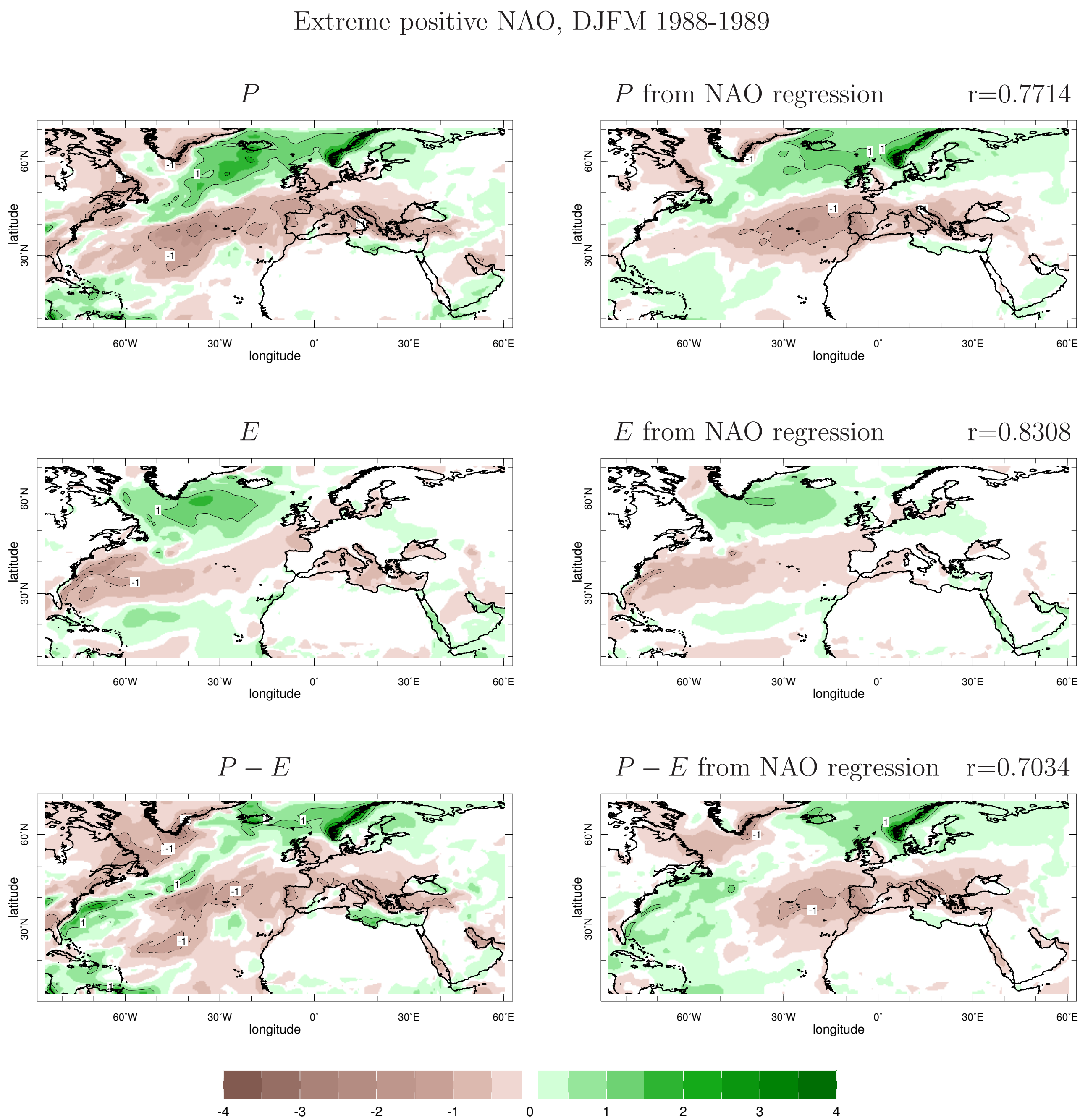

FIG. 7. The Reanalysis P, E and $P-E$ anomalies for the extreme positive NAO winter of 1988/89 (left column) and the component attributable the NAO anomaly (right column). Area-weighted spatial pattern correlation coefficients between observed and NAO-attributed patterns are shown above right panels. Units are mm/day.

Accepted for publication in *Journal of Climate*. DOI 10.1175/JCLI-D-20-0011.1.

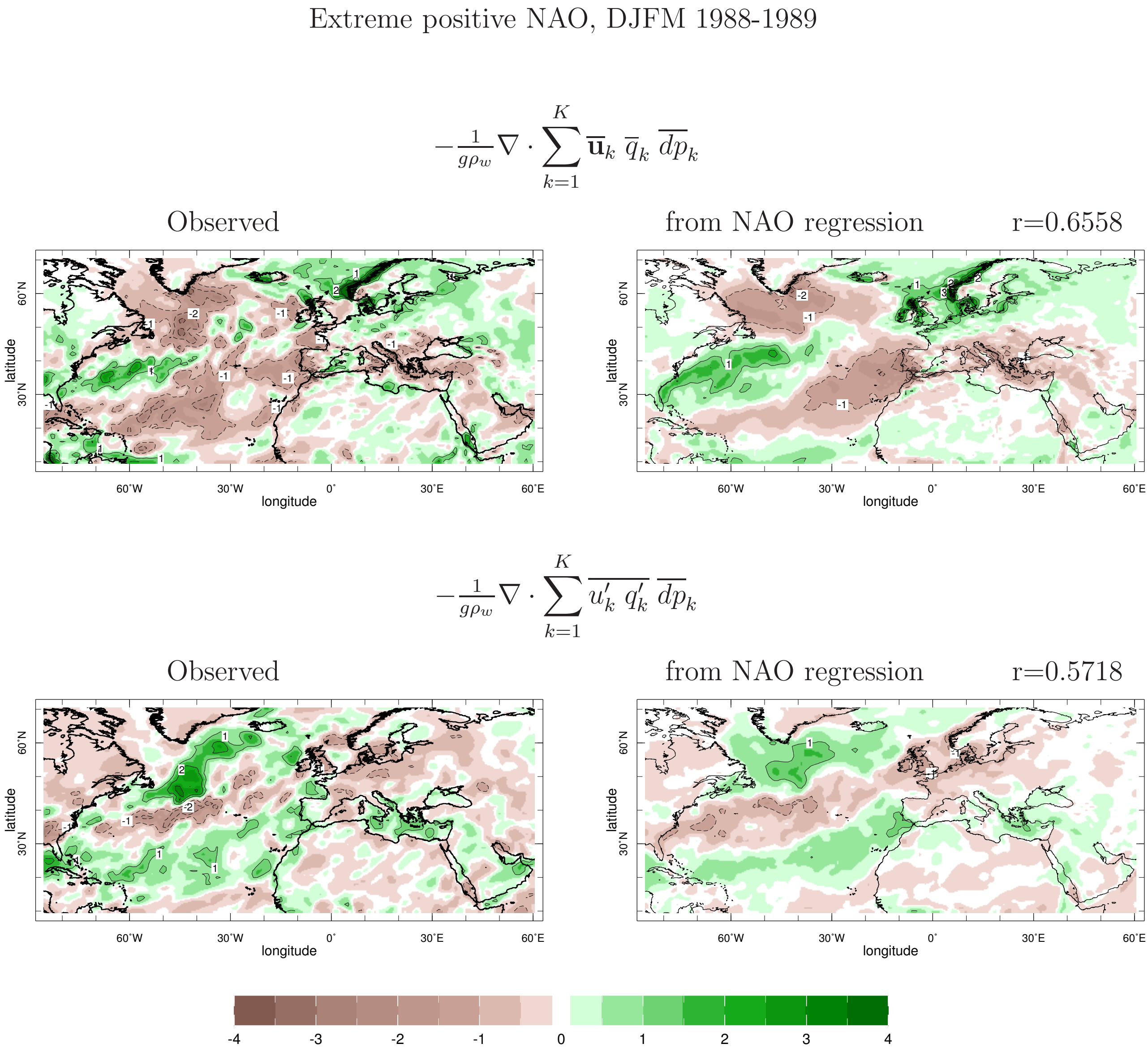

FIG. 8. The reanalysis mean flow (top) and transient eddy (bottom) moisture convergence anomalies for Reanalysis (left) and the component attributed to the NAO (right) for the extreme positive NAO winter of 1988/89.

Accepted for publication in *Journal of Climate*. DOI 10.1175/JCLI-D-20-0011.1.

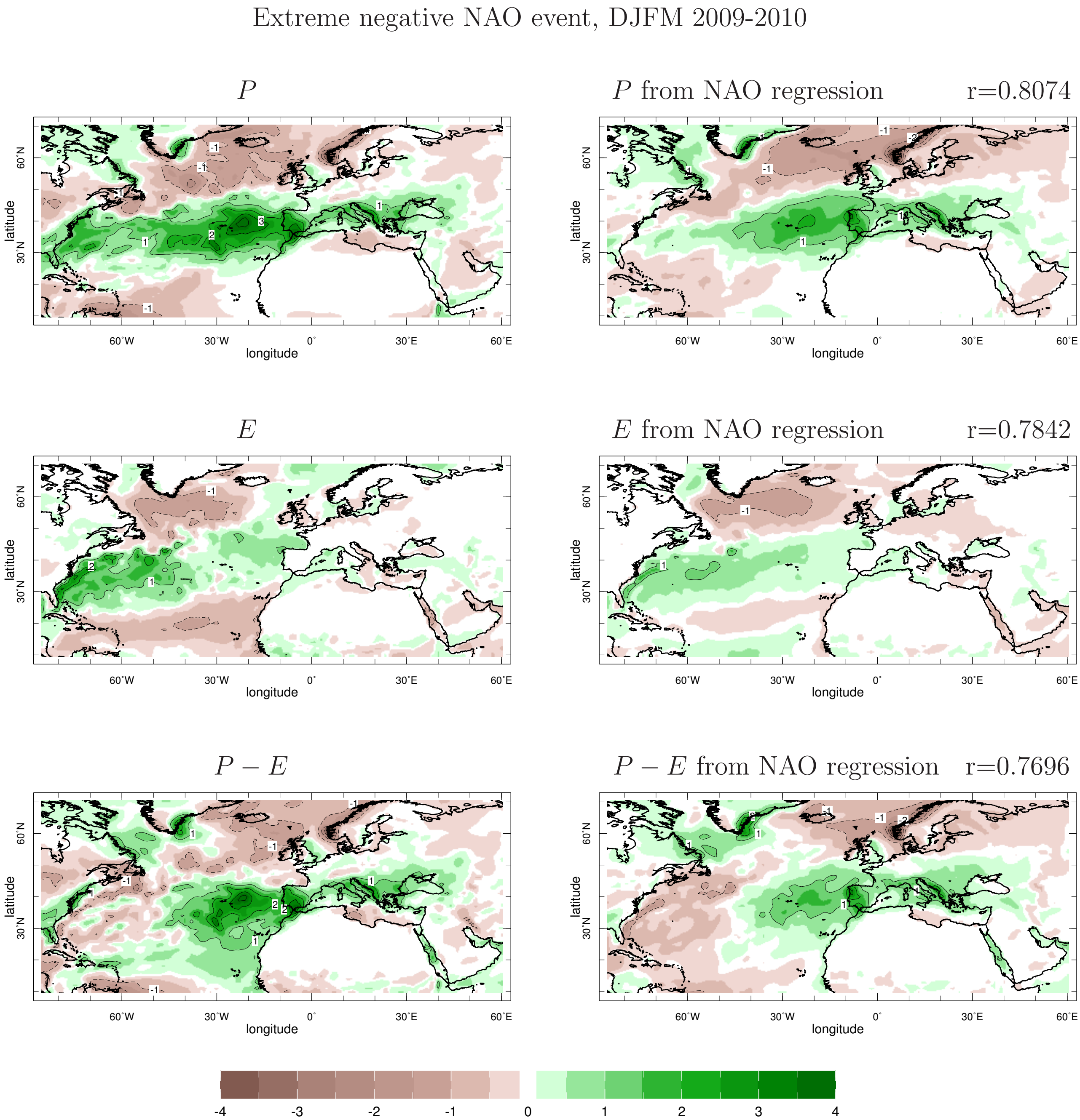

FIG. 9. Same as Figure 7 but for the extreme negative NAO winter of 2009/10.

Accepted for publication in *Journal of Climate*. DOI 10.1175/JCLI-D-20-0011.1.

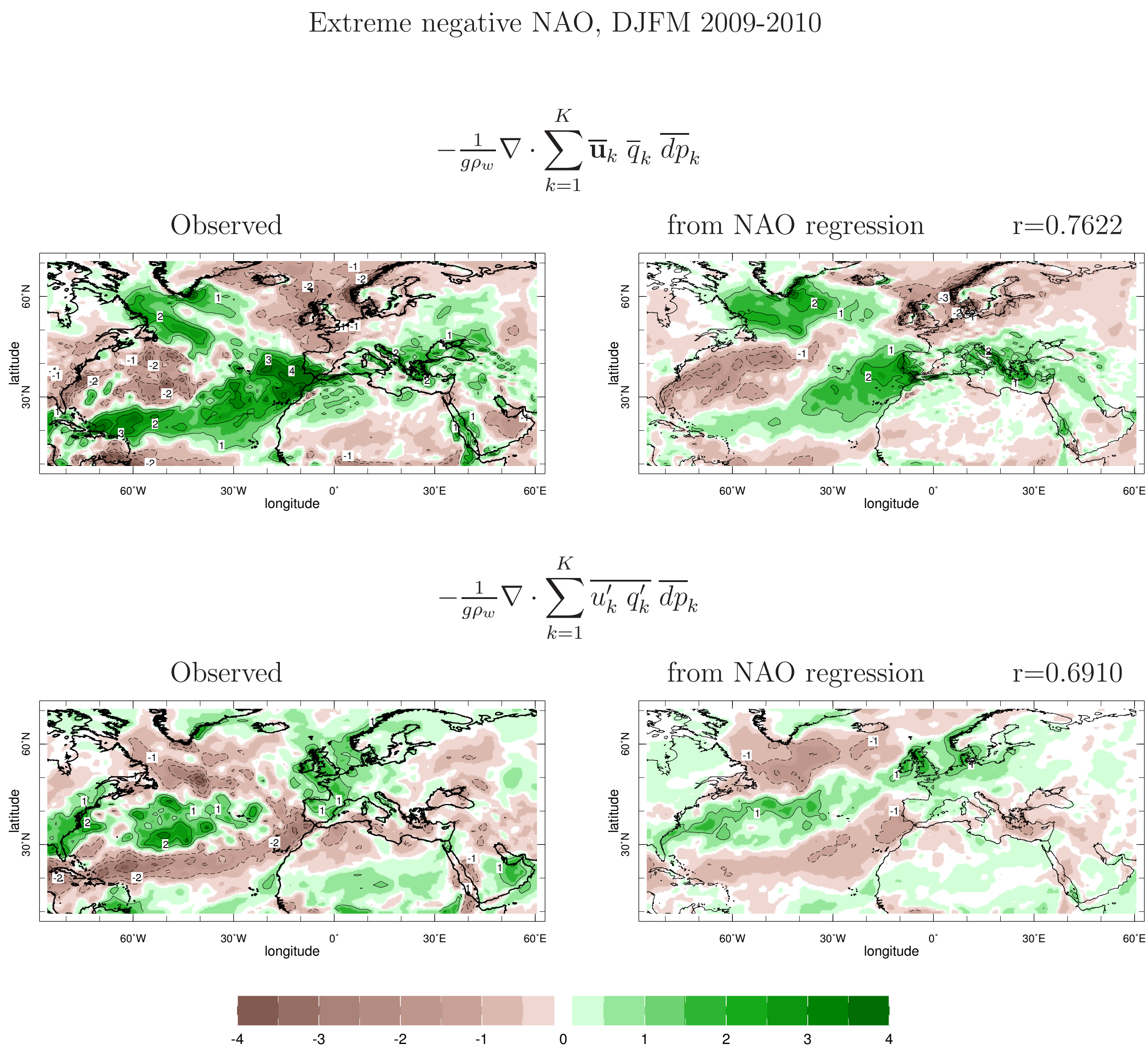

FIG. 10. Same as Figure 8 but for the extreme negative NAO winter of 2009/10.

Accepted for publication in *Journal of Climate*. DOI 10.1175/JCLI-D-20-0011.1.